

# An MLIR-based Compilation Framework for Control Flow Management on CGRAs

YUXUAN WANG, EPFL, Switzerland

CRISTIAN TIRELLI, USI, Switzerland

GIOVANNI ANSALONI, EPFL, Switzerland

LAURA POZZI, USI, Switzerland

DAVID ATIENZA, EPFL, Switzerland

Coarse Grained Reconfigurable Arrays (CGRAs) present both high flexibility and efficiency, making them well-suited for the acceleration of intensive workloads. Nevertheless, a key barrier towards their widespread adoption is posed by CGRA compilation, which must cope with a multi-dimensional space spanning both the spatial and the temporal domains. Indeed, state-of-the-art compilers are limited in scope as they mostly deal with the data flow of applications, while having little or no support for control flow. Hence, they mostly target the mapping of single loops and/or delegate the management of control flow divergences to ad-hoc hardware units.

Conversely, in this paper we show that control flow can be effectively managed and optimized at the compilation level, allowing for a broad set of applications to be targeted while being hardware-agnostic and achieving high performance. We embody our methodology in a modular compilation framework consisting of transformation and optimization passes, enabling support for applications with arbitrary control flows running on abstract CGRA meshes. We also introduce a novel mapping methodology that acts as a compilation back-end, addressing the limitations in available CGRA hardware resources and guaranteeing a feasible solution in the compilation process. Our framework achieves up to 2.1X speedups over state-of-the-art approaches, purely through compilation optimizations.

## ACM Reference Format:

Yuxuan Wang, Cristian Tirelli, Giovanni Ansaloni, Laura Pozzi, and David Atienza. 2025. An MLIR-based Compilation Framework for Control Flow Management on CGRAs. 1, 1 (August 2025), 26 pages. <https://doi.org/10.1145/nnnnnnn.nnnnnnn>

## 1 INTRODUCTION

Coarse-Grained Reconfigurable Arrays (CGRAs) are a spatial architecture composed by Processing Elements (PEs) connected in a mesh topology [1, 2]. PEs comprise ALUs and local registers, supporting arithmetic operations. Being programmable at the operation level, CGRAs present far lower overhead and much faster reconfiguration time with respect to FPGAs. Indeed, as opposed to mainstream FPGAs, CGRA typically hosts multiple configurations, one of which is selected at run-time for each clock cycle. This reconfiguration capability allows CGRAs to effectively support the acceleration of intensive parts of applications (computational kernels) defined in high-level languages (e.g., C/C++) through spatial mapping and temporal configuration. CGRAs provide a high degree of flexibility and performance, attributed to their reconfigurability and data-parallel execution model, respectively [3].

---

Authors' addresses: Yuxuan Wang, [yuxuan.wang@epfl.ch](mailto:yuxuan.wang@epfl.ch), EPFL, Lausanne, Switzerland; Cristian Tirelli, [tirelc@usi.ch](mailto:tirelc@usi.ch), USI, Lugano, Switzerland; Giovanni Ansaloni, [giovanni.ansaloni@epfl.ch](mailto:giovanni.ansaloni@epfl.ch), EPFL, Lausanne, Switzerland; Laura Pozzi, [laura.pozzi@usi.ch](mailto:laura.pozzi@usi.ch), USI, Lugano, Switzerland; David Atienza, [david.atienza@epfl.ch](mailto:david.atienza@epfl.ch), EPFL, Lausanne, Switzerland.

---

Permission to make digital or hard copies of all or part of this work for personal or classroom use is granted without fee provided that copies are not made or distributed for profit or commercial advantage and that copies bear this notice and the full citation on the first page. Copyrights for components of this work owned by others than ACM must be honored. Abstracting with credit is permitted. To copy otherwise, or republish, to post on servers or to redistribute to lists, requires prior specific permission and/or a fee. Request permissions from [permissions@acm.org](mailto:permissions@acm.org).

© 2025 Association for Computing Machinery.

Manuscript submitted to ACM

Manuscript submitted to ACM

1

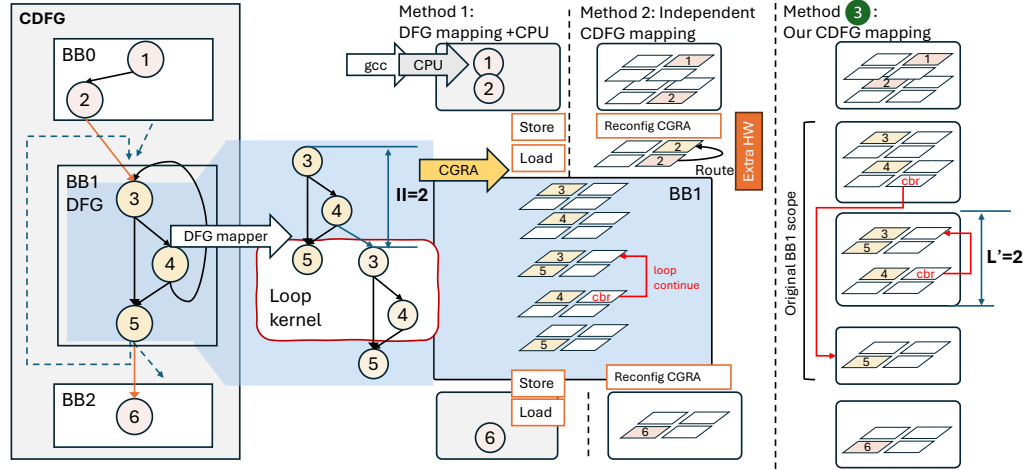


Fig. 1. Compiling applications onto the CGRA hardware. Method 1: DFG mappers fold loops to exploit parallelism, while offloading operations outside their scope to the host processor. This approach requires frequent data exchange between CGRA and host. Method 2: Independent CDFG mapping treats each basic block as an isolated DFG during compilation. Data and instruction reconfiguration are managed through dedicated hardware. Method 3: Our mapper targets CDFG compilation with branches for CFG management, resulting in no reconfiguration overhead for basic block switching.

One of the primary challenges limiting CGRA usability is the automation of application deployment to fully exploit its parallelism. Indeed, deploying applications to effectively exploit parallelism requires substantial effort [4, 5]. Most existing works simplify the CGRA compilation by limiting the compilation scope to a single DFG [6, 7], as highlighted in blue in Figure 1. A common approach for DFG mapping is through modulo scheduling (MS) [8–10]. This technique aims to overlap loop iterations, thereby minimizing the initiation intervals ( $II$ ) - the time gap between the start of consecutive loop iterations.

Although the DFG-based mapping strategy effectively exploits the loop-level parallelism [11, 12], it entirely offloads control flow management onto the host processor, as shown in Method 1 in Figure 1. Each time a kernel is deployed on the CGRA mesh, the corresponding configurations must be loaded on the hardware [13], and the input data transferred, before CGRA execution, as illustrated in Figure 2. Then, upon completion of a kernel, data must be written back into the host processor’s memory space. We herein address this shortcoming by increasing the granularity of acceleration kernels, from that of DFGs to that of entire Control Flow Graphs (CFGs).

Control Data flow graph (CDFG) mapping reduces the communication overhead between basic blocks by supporting a broader scope [14, 15], as CDFG can span multiple basic blocks and capture both control and data dependencies. Most proposed CDFG-based approaches map each DFG within the CDFG independently [16, 17], as illustrated by Method 2 in Figure 1, relying on specialized hardware for managing the ensuing branches in the execution flow. When a control dependency triggers the execution of a different DFG—such as from BB0 to BB1 in Figure 1—in these works a) new instructions must be loaded for the newly scheduled blocks, and b) the relevant data must be propagated accordingly [18]. Hence, these approaches still incur in runtime overheads and energy inefficiencies due to instruction and data reconfiguration [19].

Therefore, we argue that the limited support for complex control flows is a major limitation in state-of-the-art CGRA compilers, which are either limited in scope or adopt ad-hoc hardware solutions. Conversely, our compilation method

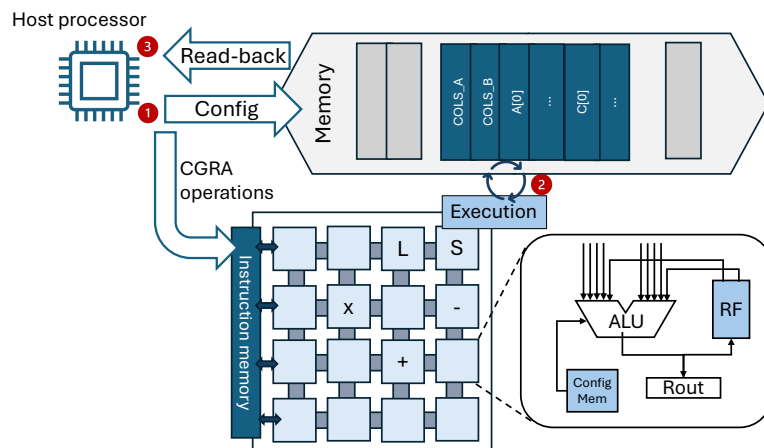


Fig. 2. Deployment of accelerated kernels on CGRA platforms. The CPU and CGRA must exchange inputs and outputs e.g. by employing a shared memory space. Moreover, configurations must be programmed in the CGRA accelerator prior to their execution.

adopts a program counter (PC)-based control flow management model. This allows the application to be compiled and configured once, eliminating the need for reconfiguration during basic block switching, as illustrated in Method 3 of Figure 1. This strategy is applicable to most CGRA architectures, which often use PC-controlled directional branches to minimize instruction memory usage [4, 20–24]. Therein, the PC-based approach is commonly limited to the scheduling of a single loop, where it allows branching back to the entry point of the loop kernel—represented by the loop continue edge in Figure 1. We instead show that such stance can be generalized by leveraging compiler transformations, in order to accommodate arbitrary control flows.

To support CDFG mapping on a PC-based controlled CGRA, a major concern is the propagation of data across basic blocks. To this end, our mapper leverages liveness analysis, [25] (traditionally used in register allocation to prevent assigning the same physical register to variables that live simultaneously) to preserve data consistency on any CFGs, regardless of their sizes or connectivity. For example, in Figure 1 value ② is live-out from BB0 and live-in to BB1. Therefore, the mapping for value ③ must be placed to access value ②. Under the mapping constraints imposed by liveness analysis across CFGs, basic block transitions are executed directly via branches without incurring any reconfiguration delays, as mapping live-in/live-out values is consistently performed in-between predecessor and successor blocks.

Our work considers a PC-based control model for any CDFG compilation that avoids reconfiguration overhead. Das et al. [26] also consider a similar hardware model, in which mappings are repeatedly sampled from a search space until data consistency is achieved. Instead, we rely on liveness analysis to draw the feasible mapping space systematically. Moreover, as noted in [26], loop-level parallelism is not supported, since a control operation must be executed at the end of each basic block to determine the subsequent execution path, thereby requiring each iteration to wait for the previous one to complete. To overcome this issue, we adopt a CFG-based transformation to adapt a new loop kernel with a loop length  $L'$  equal to  $II$ , as shown in Method 3 in Figure 1. Our approach ensures that our CDFG mapper provides the same scheduling efficiency of loops DFG mapper alternatives.

To summarize, in this work, we present a modular compilation framework for CGRAs<sup>1</sup>, offering two key advantages over traditional state-of-the-art (SoA) mapping methodologies: **(1) we extend the compilation scope to CDFG mapping on a PC-based hardware model, eliminating the reconfiguration overhead associated with basic block communication;** and **(2) we improve runtime efficiency in PC-based control model through CFG transformations to support modulo scheduling.** In more detail, our main contributions are listed as follows:

- We present an end-to-end compilation framework comprising hardware compatibility transformation, efficiency optimizations, and parameterized hardware mapping to support control flow management for various applications on a PC-based CGRA abstraction.
- We customized a `cgra` dialect in the MLIR front-end to provide direct abstraction of CDFG at the IR level, while middle-end passes rewrite unsupported hardware operations into semantically equivalent operations supported by the `cgra` dialect. This approach decouples the compilation process from specific hardware designs, discriminating hardware-agnostic and hardware-specific optimizations.
- We introduce CFG optimizations applied independently at their respective levels in the compilation stack. At a higher level, basic block fusion, a hardware-agnostic technique, simplifies the CFG by merging blocks to reduce control overhead. At a lower level, modulo scheduling—a hardware-aware mapping technique—is employed to exploit loop-level parallelism.
- We develop a mapping technology that supports CDFG mapping with control flow managed by a program counter. To maintain data consistency across the CDFG, we apply liveness analysis and formulate an integer linear programming (ILP) model to map each basic block’s DFG onto the CGRA. When the ILP model fails to find a valid solution under hardware constraints, we employ IR transformations to insert additional routing operations and/or split DFGs in order to find a valid solution.
- We compare our methods with state-of-the-art alternatives, achieving speedups of 2.12×, 1.48×, and 1.20× over EfiMap [27](PC-based CDFG mapping), SAT-MapIt [28](DFG mapping + CPU support), and Marionette [18](CDFG mapping with reconfigurable supported hardware on CGRA), respectively.

The rest of the paper is organized as follows: Section 2 reviews related work on SoA compilation methods for CGRAs. Section 3 outlines the motivation for a reconfiguration-free CDFG compilation framework. Section 4 presents the overall compilation framework, while Section 5 details hardware-agnostic transformations followed and hardware-specific IR conversion. Section 6 details the CFG transformation to enable modulo scheduling. Section 7 describes our CDFG mapping approach using an ILP model for each basic block, incorporating inter-block dependencies identified through liveness analysis. Section 8 outlines the experimental setup, and Section 9 presents our evaluation and results.

## 2 RELATED WORKS

### 2.1 MLIR

Multi-Level Intermediate Representation (MLIR) [29] comprises a front-end translating high-level languages (we herein consider C/C++) into intermediate representations (IRs). In particular, MLIR supports dialects (i.e. IR variants), allowing compiler designers to define domain-specific operations, types, and attributes [30, 31]. As a sub-project of LLVM, MLIR ensures compatibility with commonly used LLVM optimization passes and the C/C++ parsing front end. We leverage MLIR’s ability to represent both control flow and data flow at the IR level, which facilitates graph transformations in

<sup>1</sup>The code base is open-sourced in <https://github.com/esl-epfl/Compigra.git>

Table 1. Comparison with state-of-the-art CGRA mapping methods.

Features		AA-ILP[32]	SatMapIt[33]	E2EMap[34]	4D-CGRA[17]	Marionette[18]	EffiMap[26]	Ours
Memory Interface	Memory interface config	✗	✗	✗	✓	✓	✓	✓
	Automate data mapping	✗	✗	✗	✓	✓	✓	✓
Front end	ISA support	✗	✗	✗	✗	✗	✗	✓
	Imm refactoring	✗	✗	✗	✗	✗	✗	✓
DFG Mapping	DFG generation	✓	✓	✓	✓	✓	✓	✓
	instruction level parallelism	✓	✓	✓	✓	✓	✓	✓
	loop level parallelism	✓	✓	✓	✓	✓	✗	✓
CFG mapping	CFG generation	✗	✗	✗	✓	✓	✓	✓
	No extra hardware	-	-	-	✗	✗	✗	✓

the middle end. By integrating our defined hardware-specific operations into MLIR, we achieve one-to-one operation mapping to the hardware in the back end.

## 2.2 Data flow graph mapping

Table 1 includes the various features supported by SoA mappers. DFG mappers, such as AA-ILP[32], SAT-MapIt[33], and E2EMap[34] perform modulo scheduling, partially overlapping loop iterations, minimizing their Initiation Interval (*II*) to reduce runtime. Modulo scheduling handles both mapping and runtime optimization for a single loop but has limitations in managing control flow, e.g. it can only issue control-free iterations to the CGRA mesh, limiting flexibility. In these works, data transfer operations are not automated, and the DFG mappers can process only one basic block, as they do not support CFG generation, thus limiting CGRA code coverage.

Recent efforts to expand such scope include IR transformation, which merges multiple DFGs into one, employing traditional compiler optimizations such as loop unrolling and partial prediction for if-conversion [35–37]. Similarly, Dual-Issue Single-Execution (DISE) [38, 39] issues two branches (if-else clauses) within a single loop to the same PE, allowing the correct execution path to be determined at runtime based on the condition. While these methods extend the applicability of modulo scheduling, they do not ensure that every irregular loop can be successfully compiled—limiting the applications that can be accelerated by CGRAs [40]. Indeed, in these methodologies the compilation scope remains constrained, particularly for nested loops and divergent branches. Instead, we support general application compilation, enhancing mapping efficiency.

## 2.3 Control data flow graph management with reconfiguration

Compared to DFG mapping, the challenge of control management arises from compiling an entire CDFG composed of multiple basic blocks, each containing a DFG that captures computational dependencies, while minimizing control overhead. To expand the range of applications compiled onto CGRAs, approaches that integrate ad-hoc hardware components for control management have been proposed. In [11, 41], independent mapping of DFGs for each basic block is applied, while specialized hardware is incorporated for DFG switching. Dora [42] introduces dynamic binary code generation at runtime, leading to compilation and reconfiguration delays. The 4D-CGRA [17] and Marionette PEs [18] optimize the reconfiguration methods via specialized hardware design (see Table 1). 4D-CGRA [17] achieves branch prediction through entry instruction matching, requiring reconfiguration for the selected block instructions

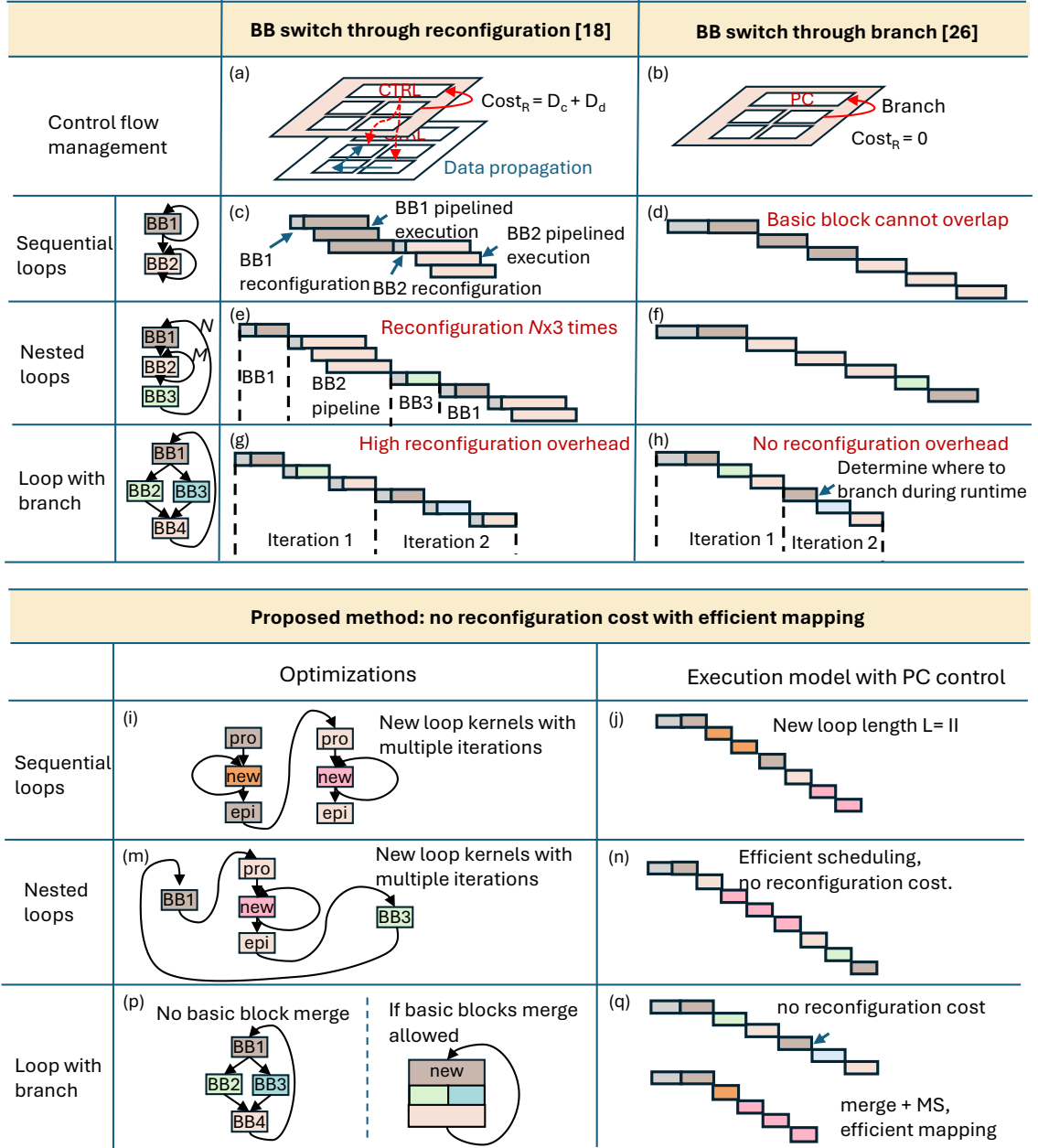


Fig. 3. Reconfiguration-based CDFG mapping incurs reconfiguration overhead, while previous PC-based mapping strategies struggle with low scheduling efficiency. Our approach achieves no reconfiguration costs and efficient mapping through compiler optimizations.

and data. The marionette PE [18] minimizes control overhead by enabling autonomous control information sharing among neighboring PEs, reducing it to a single clock cycle. However, data propagation through basic blocks remains a bottleneck for reconfiguration.

Figure 3.a illustrates the execution process for control flow management with reconfiguration. At the end of a basic block, if a control operation triggers a configuration signal from the branch operation, the control plane first reconfigures the instructions within the PEs. The instruction reconfiguration process introduces control overhead [43, 44], denoted as  $D_c$ . The required data for the newly configured basic block is either propagated from the producer PE of the previously executed block or loaded from memory, incurring additional data movement overhead, denoted as  $D_d$ . Since control flow and data flow are fully decoupled, DFG mapping is independently applied to each basic block. The innermost loop execution without control overhead is pipelined through modulo scheduling, as shown in Figures 3.c and 3.e. For sequential loops, reconfiguration is only performed during basic block switching, making it efficient with low reconfiguration overhead. However, the overhead increases significantly for nested loops. Additionally, loops with branches face a major computational bottleneck, as each basic block must be fetched separately during runtime. This limitation is illustrated in Figure 3.g.

## 2.4 Control data flow management using the CGRA program counter

CGRA PEs with program counter achieve basic block switching through branches [4, 23, 24], as illustrated in Figure 3.b. Wang et al. [45] propose an integer linear programming (ILP) model for CDFG management, aiming to minimize application runtime. However, this approach suffers from exponential complexity growth as application size increases and fails to guarantee feasible solutions for general applications. Focusing on this challenge, EffiMap [26] in Table 1 introduces a bi-directional branch in hardware to handle divergent control flows. Based on that, they introduce a heuristic scheduling method for CDFG mapping at the basic block granularity that sequentially places consumer operations to their producer PEs and stores data in internal register files. When a valid mapping cannot be found for a basic block due to register overflow or routing limitations, the algorithm backtracks to previously scheduled blocks until a feasible solution is discovered, significantly increasing compilation time. Our proposed mapping shows that CDFG can be decomposed into individual DFG mappings via liveness, as discussed in Section 7.1. Furthermore, we theoretically prove that transformations to overcome register overflow and routing limitations do not require backtracking to change established scheduling, as discussed in Section 7.4. These two strategies save compilation efficiency by decomposing the mapping complexity and avoiding rescheduling.

Moreover, their strategy results in inefficient resource utilization without exploiting loop-level parallelism. Figure 3.h illustrates this execution model for a loop with branching, where the PC dynamically controls transitions between blocks based on runtime conditions. However, since basic block execution cannot overlap under PC-based control, existing methods suffer from low scheduling efficiency. Figure 3.d and 3.f illustrate the scheduling of loops, where iterations are executed sequentially, failing to exploit loop parallelism with low hardware utilization ratio.

## 3 MOTIVATION

As discussed above, the existing CGRA compilation approaches either lack support for CDFG mapping or exhibit runtime inefficiencies [11, 18, 26]: reconfiguration-based methods incur instruction and data reconfiguration overhead during basic block transitions, while the existing PC-based method does not exploit loop-level parallelism. Driven by these limitations, we propose the development of an end-to-end compilation framework designed to address the following challenges:

**Challenge 1: The compiler must handle diverse applications with low hardware complexity for control flow management.** A general-purpose compiler should support CDFG mapping to accommodate general control flows instead of being restricted to a single DFG. State-of-the-art approaches that implement this requirement do so with

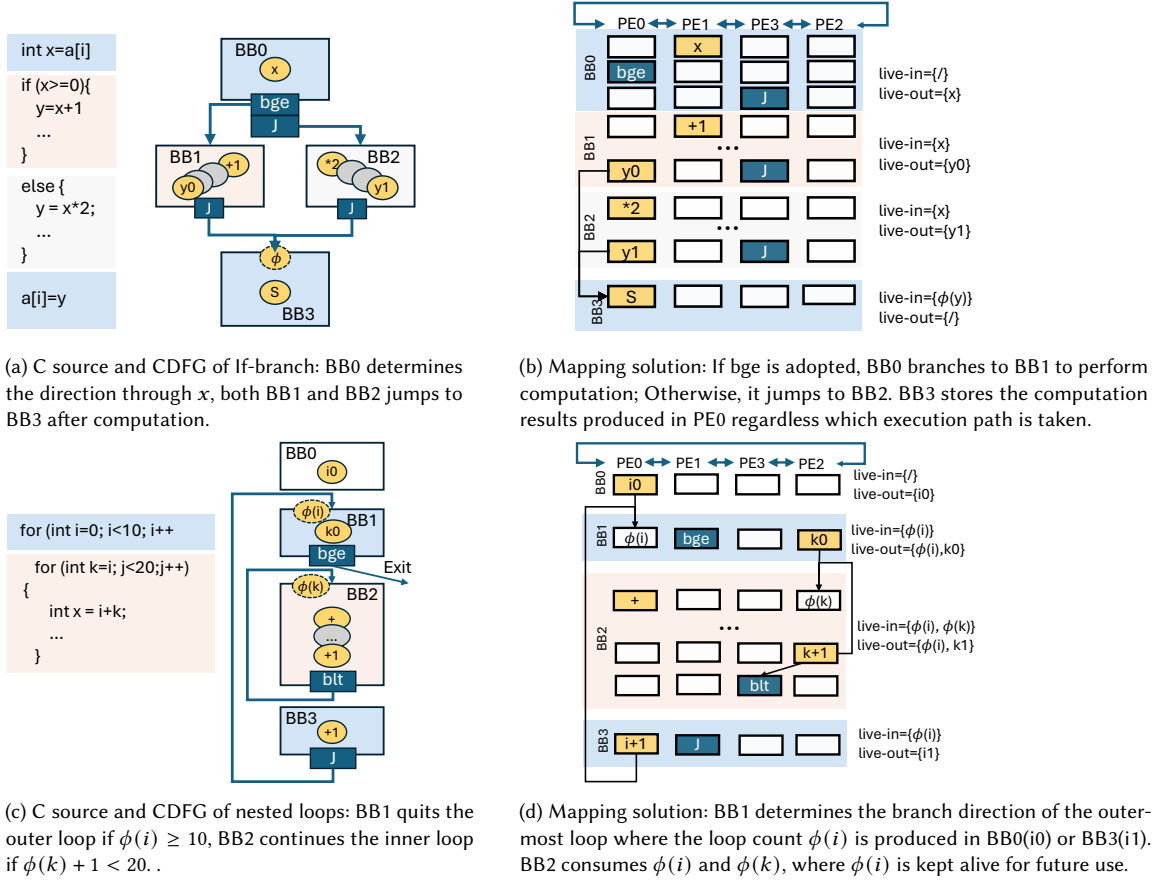


Fig. 4. Mapping CDFG onto 2x2 CGRAs with liveness analysis.

dedicated CGRA control modules that handle reconfiguration and data propagation across BBs, which incur timing penalties and area cost [18]. Compiler-based approaches can dramatically reduce both overheads, as they rely on simple program counter manipulations at run-time to handle branches [27]. However, such a strategy has only been considered for a simple control structure, such as branching to the entry point of a control-free loop. We show that, by applying liveness analysis to basic blocks to track values propagated across them, compiler-based compilation can handle complex CDFGs with nested loops and divergent branches.

Figure 4 presents examples of mapping CDFGs of applications onto a 2x2 PC-based CGRA. In particular, Figure 4.a shows a code snippet with divergent branches and its corresponding CDG. BB0 handles the divergent branch control behavior according to the loaded value  $x$ , while Figure 4.b shows a mapping solution based on liveness analysis. The loaded value  $x$  is the live-out of BB0 and live-in for BB1 and BB2. To ensure correct execution, the consumer operations in BB1 and BB2 must be placed on PEs that can access the live-in value  $x$ —specifically, PE1 for BB1 and PE0 for BB2 in the example case. Additionally, the final results of these computations, used to produce the value of  $y$ , must be mapped to the same hardware resources to maintain consistency. This design eliminates the need for explicitly selecting  $y$ 's source, as represented by the  $\phi$  function in BB3. BB3 always stores the live-in value from the exact physical location (PE0 in the example), regardless of the execution path. Figure 4.d further shows the mapping solution for a nested

loop shown in Figure 4.c, where the branch operations determine the control direction during runtime. The examples demonstrate that CDFG mapping can be decoupled into DFG-level compilation, provided inter-block dependencies are resolved using liveness analysis. With CFG constraints respected, each DFG can be compiled individually, as intra-block values do not affect the scheduling of other blocks.

**Challenge 2: The compiler should optimize for runtime efficiency.** To this end, we rely on BB fusion to increase performance, since bigger BBs offer more opportunities to exploit instruction-level parallelism. Figure 3.p illustrates an example of basic block fusion, as discussed in Section 5.1. When entire loop bodies are fused in a single BBs, loop-level parallelism can be exploited to further improve runtime efficiency. We fulfill this through CFG adaptation introduced in Section 6. Figures 3.i and 3.m illustrate such optimizations for pipelinable loops, where the adapted loop length  $L$  equals the initiation interval ( $II$ ), achieving a speedup of  $L/II$  compared to sequential execution. The optimized execution models shown in Figure 3.(j, n, and q) demonstrate higher runtime efficiency compared to both the models in Figure 3.(c, e, g) and those in Figure 3.(d, f, h).

## 4 COMPILATION FRAMEWORK

Figure 5 illustrates a bird’s eye view of the compilation process, from high-level C/C++ code to low-level assembly generation. We first rely on the MLIR frontend to perform code parsing and generate the CDFG abstraction at a high level, independent of any specific backend. Section 5.1 introduces platform-independent optimizations, aiming to reduce control overhead without relying on specific hardware requirements. Sections 5.2 and 5.3 describe hardware compatibility transformations, which are applied before any mapping-based methods to address architecture-specific differences. As a lower-level optimization, modulo scheduling of loop is instead discussed in Section 6. The modulo scheduling results, which potentially map large subgraphs of target applications, may severely constraints the overall mapping. In Section 7, we explain how we address this lack of flexibility in our framework, seamlessly integrating modulo-scheduled loops in CDFG compilation. Finally, section 7.5 discusses the register allocation process, which is performed as a final step in our methodology.

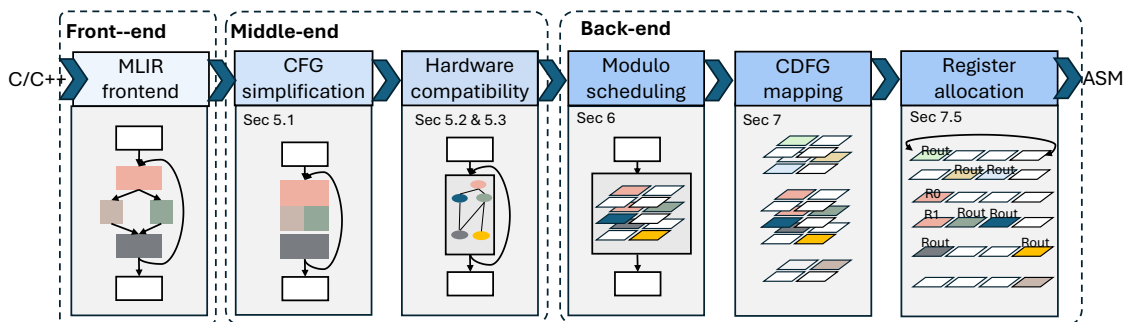


Fig. 5. Birds-eye view of the proposed CDFG compilation flow, enabling the deployment of kernel function on a CGRA mesues. The framework comprises a MLIR-based pre-processing front-end, back-end passes, ILP-based mapping, CFG transformations to support modulo scheduling and register allocation.

## 5 MIDDLE-END

The middle-end first performs CFG simplification to reduce the control overhead on the hardware, with the CDFG abstraction derived from the IR generated by the MLIR front end. Furthermore, a customized cgra dialect is developed

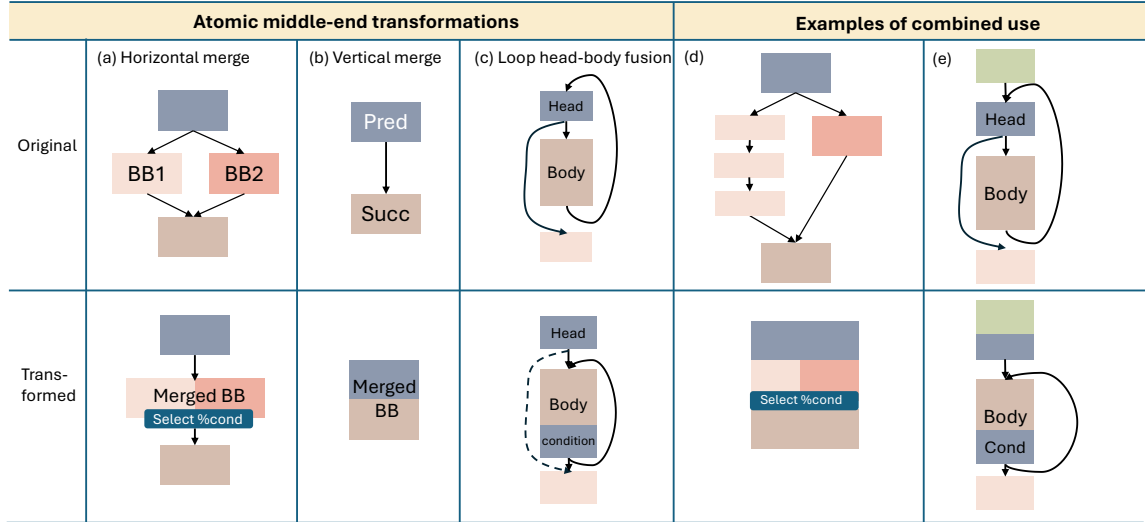


Fig. 6. CFG transformations to merge basic blocks, enabling the concurrent scheduling of the merged blocks.

to handle target-specific code generation. This design ensures compatibility between the ISA and CGRA operations, such as conditional branches and load/store instructions, while preserving a high level of abstraction.

### 5.1 Architecture-agnostic transformations

To maintain a deterministic control flow, the execution of basic blocks cannot overlap. Since basic block branching dictates execution transitions, operations from different basic blocks cannot be scheduled simultaneously. While this limitation is not a major concern in single-processor systems, where operations execute sequentially, it significantly restricts instruction parallelism in CGRA application compilation. We introduce three transformations to simplify the CFG through basic block merging. All transformations are independent and can be used in any combination.

**Horizontal merge:** Horizontal merge transforms if-execution from partial to full prediction, as shown in Figure 6.a. Therein, a predecessor basic block has two divergent successor blocks, that eventually converge at the same destination. Basic blocks can be merged if they are write-free, meaning that executing both paths only generates additional results. The final output is then determined by inserting a selection operation, which chooses the appropriate propagated values from the two merging blocks based on the runtime condition.

**Vertical merge:** Vertical merge combines two sequentially connected basic blocks into one, as shown in Figure 6.b. The predecessor has no alternative branches, and the successor has no other predecessors. Since the connection is an unconditional branch that is always taken, merging preserves the original IR functionality while allowing operations from both blocks to execute concurrently improving runtime performance.

**Loop head-body fusion:** MLIR front end generates the loop representation shown in Figure 6.c top. The loop head checks the quit condition, while the loop body control flow explicitly returns to the head before continuing iteration, which disallows modulo scheduling even for control-free loop. The transformed CFG integrates the condition check within the loop body. The head first verifies whether the loop should start, and then the body executes and decides whether to continue or exit based on the condition at the end of the iteration. Additionally, if the iteration count is

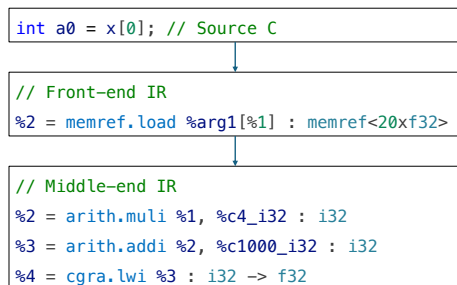
known to be greater than zero at compile time, the conditional branch simplifies to an unconditional jump to the body, ensuring the first iteration always executes.

**Combining transformations:** Our framework adopts a modular design for each atomic transformation, providing user-defined flexibility in CFG simplification. The CFG transformations are atomic and applied only when the topology matches specific patterns. This maintains compilation complexity while allowing flexible, iterative combinations for more complex CFG structures. Figures 6.d and 6.e illustrate CFG simplifications through multiple transformations. In Figure 6.d, blocks are first vertically merged, then horizontally merged with the dark pink block, and finally merged into one with their predecessor and successor. Figure 6.e shows the loop head and body fused first, followed by a vertical merge with its successor.

## 5.2 Memory operation conversion

In the high-level abstraction of the MLIR front end, a data access is represented as a memory reference argument value. Our framework translates memory references to align with the physical addresses of the corresponding data. To this end, on the CGRA side, memory access for arrays is decomposed into two steps: first, computing the element offset by multiplying the index with the stride; second, adding this offset to the array’s base address. For scalar values, only the base address is needed.

Such approach readily adapts to integration strategies where data transfers between CGRA and host are performed through a shared memory space, the most common strategy for CGRA system integration [21]. The following code snippets show the IR produced in the middle-end after memory operation conversion. In this example, %1 represents the offset value, and the constant 1000 serves as the base address corresponding to the argument.



## 5.3 IR optimization for hardware compatibility

Each CGRA implements its own ISA based on the supported operations and optimizations. Our compiler automatically eases the portability towards different architecture by providing a dedicated passes which translates illegal instructions into ones supported by a target CGRA. The translation is automated by defining a platform-specific `cgra` dialect.

For the OpenEdgeCGRA [21] instances targeted by the experiment in Section 9, the ISA translation operated by the backend rewrites the MLIR’s “compare” and “select” instructions into the CGRA’s corresponding instructions that use the zero and sign flags from the previous instruction. Similarly, we connect basic blocks by leveraging the CGRA’s specific “branch” and “jump” instructions.

The intermediate refactoring pass also checks if immediate values encoded in instructions are compatible with ISA specifications, never exceeding the size of immediate fields (e.g. 12 bits for additions for the ISA in Section 9), decomposing them across multiple operations if required. This middle-end transformation hence encompasses the

translation of read/write IR statements to loads and stores, and the rewriting of other operations with constructs supported by the target ISA. This include transformations to generate immediate value using arithmetic operations if the hardware does not support immediate fields.

## 6 IR TRANSFORMATION FOR MODULO SCHEDULING

The PC-based control model requires non-overlapping execution of basic blocks, imposing two constraints that affect runtime efficiency. First, operations from different basic blocks cannot be scheduled simultaneously. This limitation is addressed through basic block fusion, as discussed in Section 5.1. Second, control operations such as branches and jumps must be scheduled at the end of each basic block to determine control flow direction, as illustrated in Figure 4. This constraint affects loop blocks, which must complete the current data computation before executing the control operation. Thus, it hinders the exploitation of loop-level parallelism from modulo scheduling, where the next iteration starts before the current one finishes.

To overcome this latter limitation and exploit loop-level parallelism, we describe a CFG adaptation transformation that reshapes the IR, forming a new loop kernel with an iteration length  $L$  equal to  $II$ . The new loop kernel includes different parts of  $\lceil L/II \rceil$  iterations. Figure 7 illustrates the transformation of the CDFG with respect to a  $II = 2$  solution generated by a modulo scheduler. While modulo scheduling does not reduce the execution time of a single iteration, it improves the parallelization of loop iterations by minimizing the initiation interval. As a result, each iteration still executes in the loop length  $L$ , as illustrated by the dark blue nodes in Figure 7.f. However, the new loop block derived from CDFG reshaping, depicted in berry red, now encapsulates multiple iterations. This block achieves a loop length of  $L = II$ , with execution remaining non-overlapping, relying on PC-based control management.

---

### Algorithm 1: CFG adaptation w.r.t MS result

---

```

Input: loop length  $L$ ; initial interval  $II$ ;
// Init prologue and loop kernel;
for  $l=1 : \lceil L/II \rceil$  do
  Init an empty basic block  $B_l$ .
  Create DFG in  $B_l \leftarrow \mathbb{I}^l : I_k \in \mathbb{I}^l \text{ if } l \cdot II \leq t_k \leq (l+1) \cdot II$ .
  if  $l \geq 1$  then
    Set up the false branch flag of  $B_{l-1} \leftarrow B_l$ 
Set up the true branch flag of  $B_{\lceil L/II \rceil} \leftarrow B_{\lceil L/II \rceil}$ 
// Create exit blocks;
for  $l'=\lceil L/II \rceil - 1 : 1$  do
  Init an empty basic block  $B_{l'}^*$ ;
  Set up the true branch flag of  $B_l \leftarrow B_{l'}^*$ 
  Create DFG in  $B_{l'}^* \leftarrow \mathbb{I}^{l'} : I_k \in \mathbb{I}^{l'} \text{ if } t_k > (l'+1) \cdot II \forall l^* \leq l'$ .
  Connect  $B_{l'}^*$  with the finishing block unconditional jump.
  if  $l' = \lceil L/II \rceil - 1$  then
    Set up the false branch flag of  $B_{\lceil L/II \rceil} \leftarrow B_{l'}^*$ 

```

---

Algorithm 1 illustrates how CDFG-based transformations are employed to enable the integration of modulo scheduling of loops in our framework. The transformations creates basic blocks formed by grouped operations, as shown in the rectangles in Figure 7.f. The transformed CDFG is a subgraph of the overall CDFG representing the kernel. Each of its basic blocks contain operations executed in the  $II$  time period, and a new iteration will be initiated in the next block.

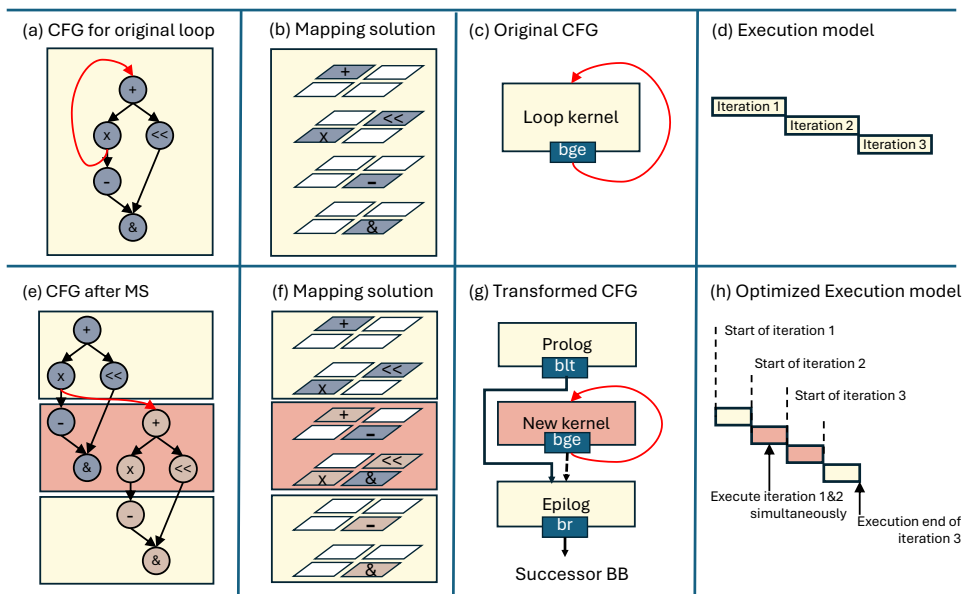


Fig. 7. CFG transformation to enable loop-level parallelism on both IR level and assembly level. (a) original CFG with a single loop; (b) mapping solution for loop length  $L=4$ ; (c) Original CFG for loop iteration; (d) original execution cycles; (e) transformed CFG with three blocks. The newly transformed loop block enables the simultaneous execution of two iterations in parallel; (f) New loop block has a reduced loop length  $L' = II = 2$ , while the original DFG is computed in two sequential iterations; (g) New CFG graph with new loop kernel encapsulates multiple iterations; (h) efficient execution cycles.

Hence, a control operation dictates whether to continue or quit the loop execution. For example, if the current iterator dictates loop exit, the controller in the prologue ( $\text{blt}$ ) in Figure 7.g branches to the epilogue and finishes the remaining operations of the current loop count. Otherwise, the PC increments one by default and passively branches to the basic block below. Such an approach allows us to support the execution of loops with variable, and even data-dependent, number of iterations. The exit blocks end up with an unconditional jump to the successor basic block of the original loop to continue the following computation.

Note that different choices for the adopted MS algorithm can be embedded in our framework. Indeed, we aim at mapping scope without compromising the obtained  $II$ , assuming a feasible schedule is provided by an existing modulo scheduling tool (we use the SATMapIt [33] compiler for the results reported in Section 9). Our framework operation mapping generated by the modulo scheduler is reused, thereby reducing compilation time. Section 7.5 discusses how to integrate modulo scheduling outcomes into the overall compilation of arbitrary CDFGs, possibly comprising multiple loops.

## 7 CDFG MAPPING

Figure 8a illustrates the scheduling methodology for mapping a CDFG, which is decomposed into DFG scheduling via liveness analysis, as detailed in Section 7.1. Inter-BB live values are stored in physical registers, with strategies for managing them discussed in Section 7.2. Each DFG is mapped using the ILP model described in Section 7.3. When the ILP model successfully generates a solution, the mapping results for values propagated across BBs are recorded for

CDFG-level integration (highlighted in the yellow table in Figure 8a). Subsequent DFGs that consume these values must adhere to the established mappings.

If the ILP model fails to find a feasible solution, a failure handler transforms the DFG by additional routing and DFG splitting. Details of this process are provided in Section 7.4. If the DFG is split in a node that is evicted to memory, the evicted values and their corresponding storage locations are recorded (highlighted in the grey table in Figure 8a), and any future references to these values are replaced with load operations from the specified memory locations. Finally, Section 7.5 describes the integration of all basic block mappings into the final assembly code generation.

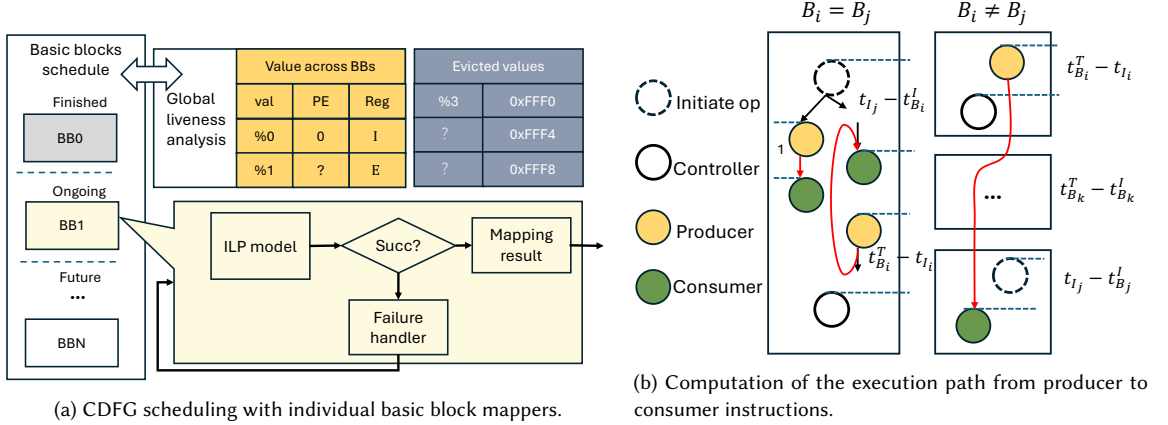


Fig. 8. Block scheme of the scheduler framework, coordinating basic block mappers through the placement of live-in/-out values propagated across basic blocks.

### 7.1 Decomposition of CDFG to individual DFGs

A CDFG consists of connected basic blocks, allowing values to propagate across them. The interface between basic blocks and the CDFG is managed through live-in and live-out values, which define how data flows between blocks. A value is considered as live-in for a basic block  $b$  if it is either used before being defined within the block or originates from a predecessor. This relationship is expressed as:

$$In[b] = use[b] \cup (out[b] - def[b]) \quad (1)$$

where  $use[b]$  represents values used within the block before being defined,  $def[b]$  includes values defined within the block, and  $out[b]$  consists of live-out values that remain live after the block. The live-out set is computed as:

$$Out[b] = \bigcup_{s \in Succ[b]} In[s] \quad (2)$$

where  $Succ[b]$  denotes the set of successor blocks. This equation ensures that the live-out values of block  $b$  are determined by the live-in values of its successors.

These equations govern value propagation across basic blocks, ensuring that data dependencies are respected by tracking the live-in and live-out values. Algorithm 2 shows this process, which involves iteratively calculating which variables are live at different program points by analyzing the CFG and variable usage patterns [25].

The computed live values indicate that they are propagated across basic blocks. Their producer PEs are initially marked as unknown, while their register index is indicated either as 'E'xternal or 'I'nternal', according to the heuristic

**Algorithm 2:** Global liveness Analysis

---

```

Initialize  $In[b]$  and  $Out[b]$  to empty sets for all
blocks;
repeat
   $changed \leftarrow false$ ;
  for block  $b$  in reverse order of CFG do
     $NewOut \leftarrow \cup_{s \in Succ[b]} In[s]$ ;
    if  $NewOut \neq Out[b]$  then
       $Out[b] \leftarrow NewOut$ ;
       $changed \leftarrow true$ ;
     $NewIn \leftarrow use[b] \cup (Out[b] - def[b])$ ;
    if  $NewIn \neq In[b]$  then
       $In[b] \leftarrow NewIn$ ;
       $changed \leftarrow true$ ;
until  $\neg changed$ ;
return  $In$  and  $Out$ ;

```

---

**Algorithm 3:** Shortest path for value propagation

---

```

Input: Instruction  $I_i, I_j$  and their belong blocks  $B_i, B_j$ 
Init  $L = 0$ ;
if  $B_i == B_j$  then
  if  $I_i \rightarrow I_j$  is back edge then
     $L \leftarrow (t_{B_i}^T - t_{I_j}) + (t_{I_i} - t_{B_i}^I)$ ;
  else
     $L \leftarrow 1$ ;
else
   $\xi_{I_i \rightarrow I_j} \leftarrow \{b_m, \dots, b_n\}$ , where  $m, n$  is the
  block index of DFS CFG from  $B_i$  to  $B_j$ ;
   $L \leftarrow (t_{B_i}^T - t_{I_i}) + (t_{B_m}^T - t_{B_m}^I) + \dots + (t_{I_j} - t_{B_j}^I)$ ;
return  $L$ ;

```

---

described in the following section (see Figure 8a). ‘E’ values are stored in the output register (Rout) of PEs, allowing them to be read by neighboring cells but preventing the PE from executing other operations until the value has been completely consumed. ‘T’ values are stored in a PE register file (RF), which does not block computation but makes the value only accessible locally to a PE, as shown in Figure 2. Once the basic block mapper (described in Section 7.3) determines the production PE from their defining block, the PE index in the table is updated to ensure that consumer(s) operation of each value can access them.

## 7.2 Value assignment across basic blocks

The decision to store a live value in external or internal registers is based on the length of the execution path from the producer to the consumer. Figure 8b illustrates the paths from the producer  $I_i$  to its consumers  $I_j$ . The left block in Figure 8b shows the live path when the producer and consumer are located in the same basic block. If the value is propagated across multiple basic blocks, its live path is determined from the producer’s execution time  $t_{I_i}$  to the end of its basic block  $t_{B_i}^T$ , through all intermediate basic blocks that must carry the value, and finally to the consumer’s execution time  $t_{I_j} - t_{B_j}^I$ . Algorithm 3 describes the computation of the shortest path  $L$ . A value produced by  $I_i$  is determined to be stored in an external register if:

$$\max L_{i \rightarrow j} \leq \theta \quad (3)$$

where  $\theta$  is a user-defined threshold, and  $j$  is the index of its consumer. This strategy prevents a PE from being blocked by long dependency paths while ensuring the value remain accessible to all connected PEs.

## 7.3 Basic block mapper

In this section, we formulate an ILP model that aims to minimize the basic block execution time through its objective function while ensuring feasibility through a series of constraints. The constraints mainly regulate the mapping behavior through four aspects: (1) accessibility - consumers must be placed where they can access the producer; (2) dominance - consumers are scheduled before the producer; (3) liveness - a value must remain in a register until it is fully consumed; and (4) sequential memory access - the memory access sequence must be preserved. The ensuing constraints are described in detail in the following.

**Global live-in constraints:** The consumer operations must adhere to specific spatial restrictions to utilize the live-ins generated outside the blocks, which are placed either in internal or external registers. If a livein variable  $v_k^E$  is located in PE  $p$  externally, then the execution units for all consumer  $p_{I_j}$  where  $I_j \in \text{Cons}(v_k)$  should be the neighbor or  $p$  itself. If the CGRA present nearest-neighbor connections, the constraint is formulated as:

$$p_{I_j} = \text{T}(p) \parallel \text{B}(p) \parallel \text{L}(p) \parallel \text{R}(p) \parallel p, \forall I_j \in \text{Cons}(v_k^E) \quad (4)$$

where T, B, L, and R represent the top, bottom, left, and right directions that are connected to PE  $p$ . Additionally, before the complete consumption of the live-in value, the PE  $p$  is blocked.

$$|p_{I_i} - p| \geq 0, \forall I_i \text{ if } t_{I_i} \leq \max(t_j), \forall t_j \in \text{Cons}(v_k^E) \quad (5)$$

Otherwise, if the value is stored in a PE's internal registers, it can only be accessed by the executed PE itself:

$$p_{I_j} = p, \forall I_j \in \text{Cons}(v_k^I) \quad (6)$$

where  $v_k^I$  is the internal live-in value.

**Dominance constraint:** The dominance constraint regulates the execution order of the operations. The execution time of  $t_{I_m}$  an operation  $I_m$  should be before its consumer in the same basic block, notated as  $t_{\text{Cons}(I_m)}$ :

$$t_{I_m} \leq t_{\text{Cons}(I_m)} - 1 \quad (7)$$

**Access constraint:** Operations should be assigned to physical PEs. In a CGRA configuration with  $R$  rows and  $C$  columns, the placement  $p_{I_m}$  of operation  $I_m$  cannot exceed the CGRA size:

$$0 \leq p_{I_m} \leq RC - 1 \quad (8)$$

The consumer should access the producer's result, which is constrained by the hardware connectivity. If the CGRA is grid-connected,  $p_{I_m}$  has to be the neighboring PE of the producer units  $p_{I_n}$ :

$$p_{I_m} = \text{T}(p_{I_n}) \parallel \text{B}(p_{I_n}) \parallel \text{L}(p_{I_n}) \parallel \text{R}(p_{I_n}) \parallel p_{I_n}, \forall j \in \text{Prod}(I_n) \quad (9)$$

**Liveness constraint:** An operation executed afterward in the same PE would overwrite the pre-produced value. This constraint ensures the liveness of the produced results of operation  $I_i$  before its consumption by  $I_j$ :

$$|p_{I_k} - p_{I_i}| > 0 \forall I_k \in \mathbb{I}, \text{ if } t_{I_i} \leq t_{I_k} < t_{I_j} \quad (10)$$

where  $\mathbb{I}$  is the full operation sets. This constraint block PEs' use until it get consumed inside one basic block.

**Control constraint:** An operation must be executed after the initiation time  $t^I$  of the basic block it belongs to, and before the control operation at the end of the block:

$$t^I \leq t_{I_m} \leq t_{\text{control}}, \forall m \quad (11)$$

**Global live-out constraints:** The basic block must keep its live-out value inside the registers. If the value is externally live-out, it should not be overwritten:

$$|p_{I_i} - p| > 0, \forall I_i \text{ if } t_{I_i} \geq t_j \quad (12)$$

where  $p$  is the PE where the live-out exists, and  $t_j$  is its produce time.

For the live-out value placed in internal registers, the total number cannot exceed the available register numbers  $N_r$ :

$$\sum_{I_i \in \text{liveout}} (p_{I_i} = p) \leq N_r, \quad \forall p \quad (13)$$

where  $p_{I_i}$  is the scheduling result for an operation  $I_i$  which produces a live-out value.

**Memory consistency constraints:** To maintain memory consistency, a store operation  $I^S$  acts as a barrier that enforces ordering between load operations executed before and after it. Specifically, all load operations preceding the store must be completed before the store operation, and the store operation must be completed before any subsequent load operations. This is expressed as:

$$t_{I_m}^L < t_{I^S} < t_{I_n}^L, I_m \in \mathbb{I}_{\text{before}}^L \ \& \ I_n \in \mathbb{I}_{\text{after}}^L \quad (14)$$

where  $\mathbb{I}_{\text{before}}^L / \mathbb{I}_{\text{after}}^L$  represents load operation sets executed before/after  $I^S$ .

**Objective function:** The final objective the ILP model is to minimize the basic block execution time, which is

$$\min t_{\text{control}} - t^J \quad (15)$$

The objective of the optimization is to maximize runtime efficiency for the execution of the basic block. The constraints, defined in Equations 4–14, govern the placement of operations to ensure correct execution semantics. Based on these constraints, the ILP model generates both the temporal and spatial mappings for each operation within the basic block. If the scheduled operations produced value across BBs, the placement is updated in the live value table, as shown in the example of Figure 8a.

#### 7.4 IR transformation to handle ILP failure

The ILP model does not guarantee the existence of a solution due to CGRA hardware constraints. We herein discuss a strategy that counters two key sources of unfeasible solutions: routing limitations and register overflow. Figure 9 illustrates the IR of a block facing both failure scenarios. Figure 9b shows the pre-scheduling operations with live value placements, while the first row of Figure 9a indicates their locations. Value %4 encounters routing limitations as %0 is only accessible by PE0, while PE0 cannot reach PE3 for %1. This conflict is resolved by inserting a move operation (add %1, 0) to route %1 from PE3 to PE1. Value %5 cannot use %2 and %3, as they are stored in different PEs' internal registers. PE3 is blocked from popping %3 until its external register value is consumed. To address this, %3 is evicted to memory, and a load operation is inserted. Figure 9c shows the transformed IR with the additional move and load operations, enabling a feasible mapping solution.

Routing limitations arise when connectivity constraints prevent consumers from accessing values produced and stored in specific PEs. Register overflow occurs when internal or external registers conflict with live values, requiring one to be evicted to memory. While splitting the DFG by inserting load-store pairs can always resolve these issues, it may introduce significant overhead. To address ILP model failures efficiently, we employ a *max-try* or *roll-back* strategy. If a consumer cannot access a producer, up to  $N$  move operations are inserted. If a feasible solution is still not found after  $N$  moves, the IR is rolled back, and a load-store pair is inserted to resolve the conflict. The threshold  $N$  depends on the load and store overhead, with  $N \leq D - 1$ , where  $D$  represents the length of the longest routing path in the CGRA architecture. For example, in a  $2 \times 2$  CGRA, routing from PE0 to PE3 results in  $D = 2$ .

Handling failures with additional move operations or load-store pairs does not require re-scheduling blocks that already have solutions. Indeed, a basic block transformation can only affect other basic blocks by altering the result of liveness analysis, which involves the value propagated through basic blocks, as discussed below.

If a value  $v$  leads to the ILP model failure is used and defined only inside the basic block  $i$ ,  $v \notin use[b_j] \ \forall j$ , resulting  $v \notin In[b_j] \ \forall j$ . Moreover,  $v \notin In[b_i]$  because  $v \notin use[b] - def[b]$  according to Equation 1. The value is in this case not recorded in the live value across BBs and cannot affect the other basic blocks.

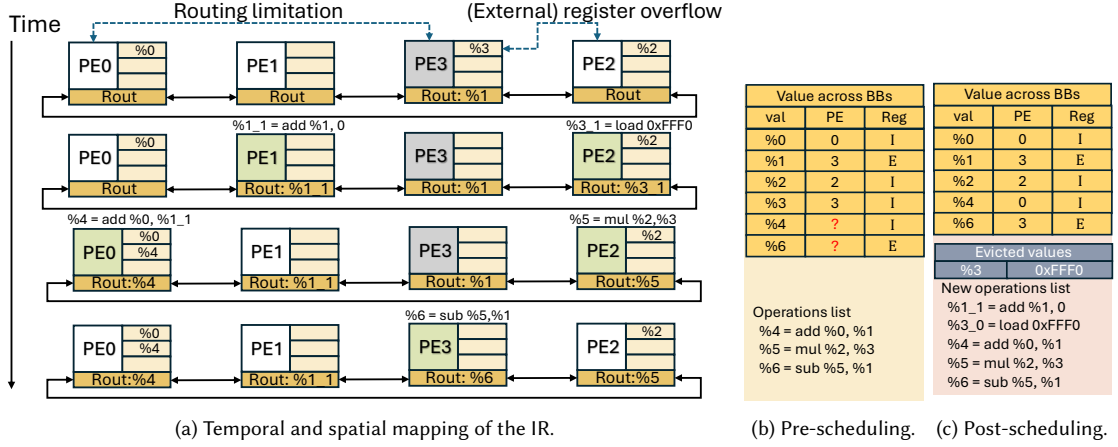


Fig. 9. DFG transformation for converting an ILP model to find a feasible solution. The transformation takes into account limited routing and register resources (a) to schedule additional stores/loads and move operations between registers and memory (b-c).

$v$  may instead be defined and used in different blocks. For a block  $b$ , if move operation  $I_m$  are inserted to route the value  $v$  from its original producer  $I_p$ , result of  $I_m$  replaces the use of  $v$ . However, the set  $use[b]$  still includes  $v$  through  $I_m$ . Therefore, the live-in set defined in Equation 1 remains unchanged, preserving the results from liveness analysis and ensuring no impact on other blocks' scheduling.

In case a load and store are inserted for  $v$ , let's define its consumer as  $b_j$  and its producer block  $b_i$ . For the producer block, the define and use sets remain the same:  $use\{b_i\}' = use\{b_i\}$ , and  $def\{b_i\}' = def\{b_i\}$ . For the consumer block,  $use\{b_j\}' = use\{b_j\} - v$ , and  $def\{b_j\}' = def\{b_j\} + v_0$ , where  $v_0$  is the loaded value to replace  $v$ . This transformation updates the value across BBs by removing  $v$  from BB propagations according to Equation 1. Figure 9c shows evicting value % 3 from the register to the memory. This still abides to the scheduler results, as it represents a relaxation of the constraints in Section 7.3, meaning the previous scheduling remains valid except a store operation need to be inserted after the produce of the split value %3. This process involves identifying an available neighboring PE after the split value has been produced. If no available PE exists, additional cycles are introduced to accommodate the store operation, without the need for re-scheduling.

## 7.5 Composing modulo and CDFG scheduling

When modulo scheduling of loops is performed before CDFG transformations, the allocated PEs and registers for the live-in and live-out values of the scheduled block are first recorded as in the table in Figure 8a. This ensures that subsequent blocks maintain consistency with the modulo scheduling results, so that there is no need to run the BB scheduler for the mapped blocks, as they have already been resolved.

After the scheduling for all blocks is completed, the top-level scheduler merges the mapping results of all basic blocks to obtain the CDFG mapping solution. In particular, the top-level scheduler assigned starting times ( $t^J$  in Section 7.3) to each basic block. The concatenated scheduling result ensures the data consistency through the global live-in constraints (constraints 4- 6, again in Section 7.3) and global live-out constraints (constraints 12 - 13).

## 7.6 Back end

As a final step for CDFG mapping, register allocation is performed. Operands from neighbor PEs are retrieved from their output registers, eliminating the need for register allocation in local RF when data is routed from one PE to another. Internal register allocation is performed per-PE, similarly to state of the art approaches such as [46]. This step involves constructing a liveness graph for each PE and applying graph coloring to assign distinct physical registers to values that interfere with one another. After register allocation, a final rewriting pass converts the MLIR code to the needed input for the CGRA assembler. During the MLIR-to-CGRA assembler conversion, redundant jumps to basic blocks placed immediately afterwards in the instruction placements are removed. The assembler is then translated into binary form for execution on the target hardware.

## 8 EXPERIMENTAL FRAMEWORK

**Target CGRAs.** Across experiments, we considered as architectural instances of the OpenEdge CGRA template [21] of varying mesh sizes. The CGRA adopts a minimal yet Turing-complete ISA, which allows for flexible and efficient execution of a wide range of computational tasks while maintaining low hardware complexity. The control flow is managed by an unconditional jump and four conditional branches with predicates equal (EQ), not equal (NE), greater or equal than (GE), and less than (LT). The hardware is synthesized in 250MHz with 65nm technology and a cycle-level software simulator is provided to verify the functional correctness and evaluate the runtime metrics.

Table 2. Characteristic of our framework compared to SoA alternatives

Works	SW Scope	HW requirements for control flow management
EffiMap [27]	CDFG	bi-directional jumps, Constant register files
Marionette [18]	CDFG	Reconfiguration unit, CFG control network
SatMapIt [28]	DFG	External CPU for CFG management
<b>Ours</b>	CDFG	/

Table 3. Benchmark Categories and Attributes

Types	Benchmarks	CFG Attributes	I/O Data sizes
Convolution	conv3d	6-level nested loops	3x15x15 input, 2x5x5 kernel
	conv2d	4-level nested loops	12x12 input, 3x3 kernel
	conv1d	3-level nested loops	1x64, input 1x3 kernel
Linear Algebra	bicg	1-level+ 2-level nested loops	20 x 30 data
	gemm	4-level nested loops with control	3 10x10 matrix
	symm	3-level nested loops with controls	3 10x10 matrix
	2mm	2 sequential 3-level nested loops	4 8x8 matrix
	3mm	3 sequential 3-level nested loops	7 4x4 matrix
Signal Processing	fir	2-level nested Loops with branches	1x16 input, 1x5 coefficients
	gsm	Loop with multiple branches	1x50 arrays
	sha_transform	4 sequential compute intensive loops	1x16 data, 1x80 weight

**SoA methods.** We compare our method and target platform with state-of-the-art mapping methods and their respective hardware requirements in Table 2. EffiMap [27] supports CDFG mappings with PC-control, while bi-directional jumps are implemented by a dedicated control unit. Constant register files are utilized to generate and manage constant values. Conversely, we achieve these functionalities entirely through software techniques, as explained

in Section 5.3. A bi-directional jump is replaced with a one-direction conditional jump, the false case is executed with an unconditional jump, and constants are generated through combinations of arithmetic operations. Marionette [18] also supports CDFG but requires complex hardware components, including a reconfiguration unit and a CFG control network to propagate the DFG switch decision. SatMapIt [28] only focuses on DFG mapping, leveraging external CPU for CFG management. We consider this methodology both as a stand-alone baseline strategy, and as the modulo scheduler employed in our framework.

**Benchmarks.** We consider a representative set of benchmarks including convolution for deep learning, linear algebra from PolyBench [47], and signal processing from MiBench [48]. The benchmarks, along with their data sizes and CFG attributes, are detailed in Table 3.

## 9 RESULTS

We evaluate our approach from multiple viewpoints. First, we showcase that our CDFG stance effectively increase the compilation scope with respect to DFG-based alternatives. Then, we report the effect of the devised CFG-based optimizations on compile time. Furthermore, we discuss the run-time performance improvements deriving from each optimization technique introduced in this work. Finally, we compare our compilation framework with state-of-the-art approaches and their respective target platforms, demonstrating that our method offers higher mapping efficiency while requiring minimal hardware for controlling execution.

### 9.1 IR scope analysis

Figure 10 illustrates the applicable scope of DFG mappers, where the blue sections represent operations for control-free loops and the orange sections indicate operations outside the innermost loops, for which control flow considerations are required. The numbers and ratios shown in the pie charts indicate the count of operations and their proportion

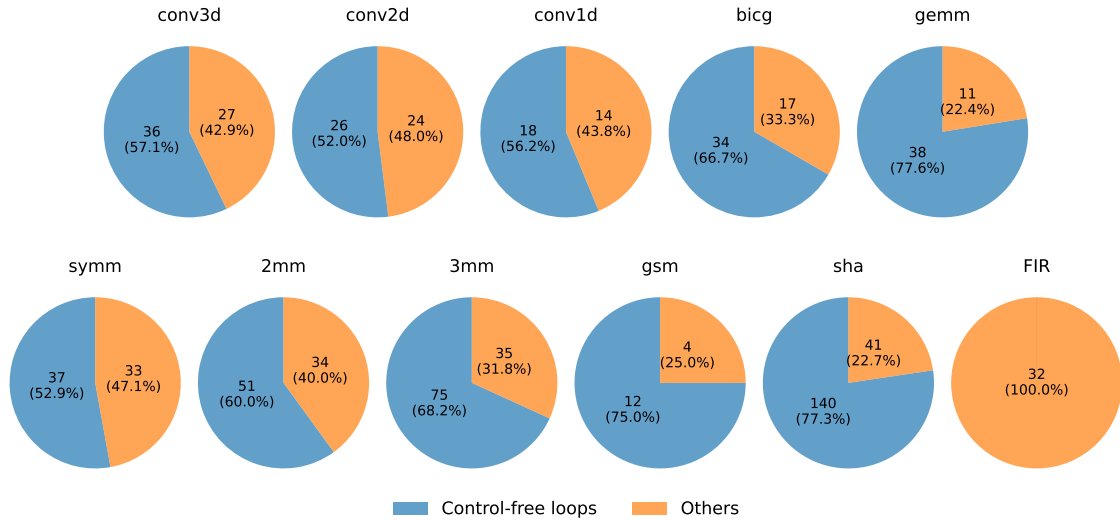


Fig. 10. Break-down of operations in the considered benchmarks, reporting the percentage of operations belonging to the most internal loops. Only those can be mapped on CGRA using DFG-only strategies, while our approach allows for the entirety of kernels to be CGRA-accelerated.

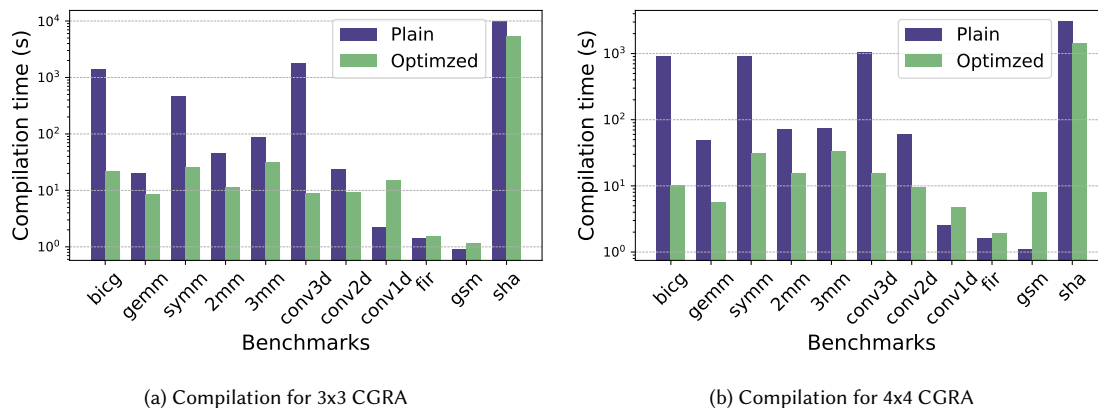


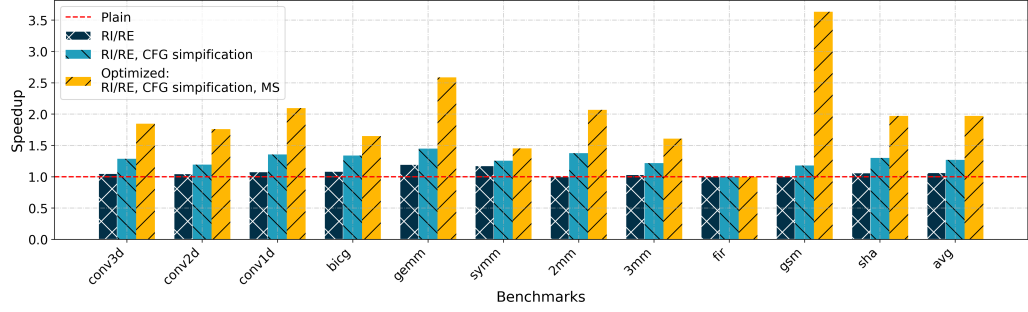
Fig. 11. Compilation time comparison on Intel(R) i7-13700H. Plain indicates mapping for IR generated by MLIR front end, and Optimize shows the compilation time where the IR undergoes all optimizations supported in the framework. Lower values are better.

relative to the total number of operations in each application. Results indicate that the scope and complexity of CGRA kernels can be effectively increased by considering control flow. The CFG of FIR cannot be simplified to include a control-free loop that is targetable by DFG mappers, which must be mapped by a CDFG compiler. Moreover, they hint that a DFG-only approach can result in high overheads for the orchestration of CGRA configuration and input/output data transfers, as discussed in Section 9.4. Such overheads are entirely waived in our proposed strategy, as a single configuration is required for supporting the acceleration of the entirety of each kernel.

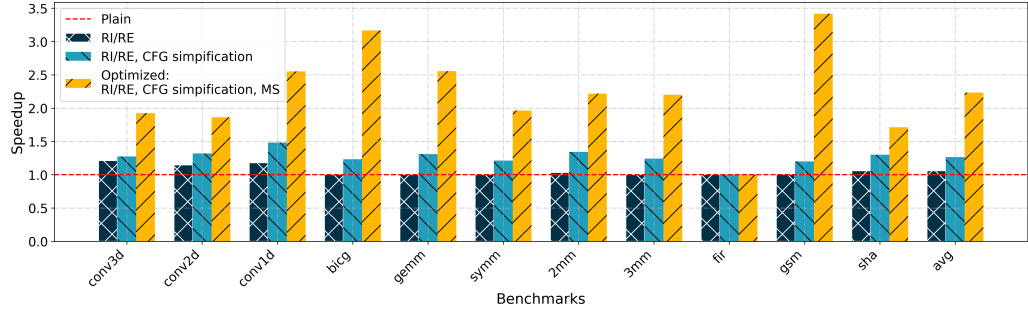
## 9.2 Compilation time

The compilation time encompasses the whole compilation process required to map an application, including the front, middle, and back end for IR transformation, operation mapping, and register allocation for assembly generation. Figure 11 illustrates the total compilation time targeting  $3 \times 3$  and  $4 \times 4$  CGRAs. In the plain compilation flow, operation mapping is performed directly on the IR generated by the MLIR front end. In contrast, the optimized flow processes the IR through CFG simplification (Section 5.1) and adaptation with modulo scheduling (Section 6). CDFG mapping is decomposed in our methodology into the mapping of its constituent basic blocks. Therefore, the total mapping time is primarily influenced by two factors: the number of operations within individual basic blocks and the total number of basic blocks. Mapping complexity increases exponentially with the number of operations in a basic block, making blocks with large DFG sizes the primary contributors to overall mapping time. Additionally, the presence of multiple basic blocks with high mapping complexity further extends compilation time. For instance, the gsm benchmark contains six basic blocks, each with fewer than five operations, resulting in relatively fast compilation. In contrast, sha comprises eight basic blocks, each containing over 25 operations, which significantly increases mapping time.

Operation mapping dominates the overall compilation time, whereas the time spent on IR transformation and register allocation is negligible. This is exemplified by the FIR benchmark, whose CFG cannot be simplified by our approach. Hence, the observed increase in compilation time is attributed solely to IR transformation, which contributes only a few milliseconds. The optimized implementation exhibits longer compilation times compared to the plain version for the conv1d benchmark, with compilation overhead increasing by several seconds. In the case of conv1d, the control-free kernels contain small counts of operations with reduced dependencies, making the plain version easier to find a solution.



(a) Applying optimizations on a 3x3 CGRA.



(b) Applying optimizations on a 4x4 CGRA.

Fig. 12. Impact of register allocation for live values, CFG simplification, and modulo scheduling across various CGRA sizes. RI/RE denotes our optimized Register Internal/External placement strategy. The use of CFG simplification and modulo scheduling is indicated when the respective technique is applied. Higher values are better.

The modulo scheduler performs more extensive exploration to identify initiation intervals that can exploit the available parallelism. Indeed, most optimized compilation flow achieves faster compilation than the plain methodology. This improvement stems from CFG simplification, which restructures the CFG to be amenable to modulo scheduling. The SAT-based modulo scheduler employed in our flow reduces mapping time for computation-intensive loop kernels.

### 9.3 Impact of optimizations on run-time

Three factors influence the runtime efficiency of the mapping results produced by the proposed framework, ranked in order of their impact: (1) the register attributes used to assign inter-basic-block values, as discussed in Section 7.2; (2) CFG simplification techniques that change the CFG structure, detailed in Section 5.1; and (3) transformations based on modulo scheduling to enable loop-level parallelism, described in Section 6. Figure 12 illustrates the performance improvements achieved through different combinations of optimizations. Plain and Optimized compilation settings are defined as in Section 9.2— in Plain no optimization is applied, while in Optimized all are employed. Additionally, we evaluate intermediate configurations that (1) apply only values allocations in both internal and external registers, and (2) apply CFG simplifications further.

The placement of values propagated across basic blocks significantly impacts convolution and linear algebra benchmarks, as these workloads carry high data dependencies through nested loops for computing memory addresses. For a 4×4 CGRA running convolutional benchmarks, selectively placing partial variables in external registers expands the access range, resulting in an 6.6% acceleration gain on average. Combinational use of the CFG transformations

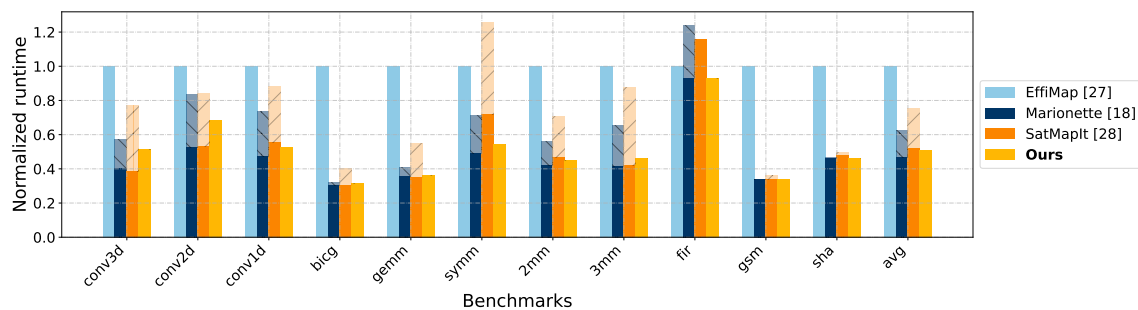


Fig. 13. Evaluation of normalized runtime across different architectures. EffiMap and our method employ a single CGRA configuration for supporting entire kernels, while Marionette and SatMapIt require reconfiguration during basic block switches, with the reconfiguration overhead shown as a semi-transparent color. Lower values are better.

simplifies the control flow, particularly in `gsm`, where five blocks are merged into a single self-iterating loop. This CFG simplification enables multiple blocks to be consolidated, allowing merged operations to be scheduled simultaneously. As a result, acceleration gains of 26.8% and 26.4% are achieved on  $3 \times 3$  and  $4 \times 4$  CGRAs, respectively. For `conv1d` on a  $4 \times 4$  CGRA and `gemm` on a  $3 \times 3$  CGRA, performance improvements reach up to 48% and 45%, respectively. Loops with lower nested levels such as `gsm` and `gemm` obtain 316% and 255% runtime faster on a  $4 \times 4$  CGRA. On average, modulo scheduling folds the innermost loop, achieving 197% on  $3 \times 3$  and 223% acceleration on  $4 \times 4$  CGRAs, indicating  $L \approx 2 * II$  achieved by the modulo scheduler. CGRAs with larger grid sizes achieve higher speedups, as the presence of more hardware resources enables higher parallelism. In general, the introduced optimization are highly beneficial on all considered benchmarks. FIR is an outlier, as its CDFG structure presents a write operations in one branch inside an innermost loop, which disallow basic block merging.

#### 9.4 Comparison with state-of-the-art methodologies

Figure 13 shows the execution runtime of benchmarks on  $4 \times 4$  CGRAs for the methodologies described in Table 2. Results are normalized with respect to EffiMap [26], which supports CDFG mapping without reconfiguration overhead. Marionette [18] also supports CDFG mapping but involves reconfiguration time for basic block switching, depicted in semi-transparent dark blue. Since in the case of SatMapIt [28] only a portion of benchmarks can be CGRA-accelerated, we optimistically assume that non-CGRA code runs on a processor with an IPC (instructions-per-cycle) equal to 1. In Figure 13, non-CGRA run time plus CGRA configuration overhead for SatMapIt is depicted in semi-transparent orange.

Our compilation approach achieves the lowest compilation runtime across all benchmarks, as shown in Figure 13. We attain average speedups of  $2.12\times$ ,  $1.48\times$ , and  $1.20\times$  over EffiMap [26], SAT-MapIt [28], and Marionette [18], respectively. EffiMap does not fully exploit the optimization spaces during the compilation process: it relies on dedicated hardware to support instruction-level parallelism, but neglects loop-level parallelism opportunities. However, loop-level parallelism is critical for optimizing runtime efficiency for CGRA, as discussed in Section 9.3, where modulo scheduling achieves  $L \approx 2 * II$ . Our CFG adaptation creates new kernels with loop length  $L' = II \approx 0.5 * L$  on average. EffiMap achieves faster runtime for FIR because modulo scheduling cannot be performed due to the presence of non-mergeable branches inside an innermost loop. Our compilation method outperforms theirs because their heuristic strategy does not optimize for the shortest basic block runtime, leading to suboptimal solutions.

When the computational workloads dominate the benchmarks with control-free, non-nested loops, both SATMapIt and Marionette achieve performance comparable to our method, as the runtime reconfiguration overhead becomes negligible. This is shown in benchmarks such as `gsm` and `sha`. However, both SatMapIt and Marionette experience significant reconfiguration overhead for nested loops. For example, a `conv3d` application with an input tensor of dimensions  $D \times H \times W$  (depth  $\times$  height  $\times$  width) and a kernel of dimensions  $d \times h \times w$  would require reconfiguration  $D \times H \times W \times d \times h$  times—the number of branches to execute the innermost loop over the kernel width  $w$ . Even if the reconfiguration time is optimized to take only a few clock cycles, the large number of reconfigurations still introduces a substantial overhead. For `conv2d` and `conv3d`, the computation time is faster for Marionette and SatMapIt than for our approach, as in these methods, no live-in / live-out values must be maintained across basic blocks. Nonetheless, our approach still outperforms both when reconfiguration time is accounted for, because the entire benchmark can be mapped as a single computational kernel.

In conclusion, our compilation framework outperforms methodologies that rely on hardware reconfiguration units by eliminating the need for reconfiguration during basic block transitions. It also surpasses other PC-based control models through CFG reshaping, which enables effective support for modulo scheduling.

## 10 CONCLUSION

By combining efficiency and reprogrammability, CGRAs can support the acceleration of computationally intensive edge applications. The key to their mainstream adoption is the availability of a compilation framework enabling the automatization of the deployment of complex compute kernels on available hardware resources.

Against this backdrop, we have proposed in this paper a novel end-to-end framework that, by leveraging and extending the MLIR infrastructure, is able to generate CGRA assembly from source code. We broadened the scope of CGRA scheduling by considering control flow as well as data flow in the compilation process, showcasing how this approach can be employed to efficiently compile kernels. Moreover, our framework supports compilation for applications with arbitrary control flows without dedicated hardware support. The introduced CFG-based optimizations lead to speedups of 1.96x and 2.23x on 3x3 and 4x4 CGRAs, respectively, resulting in, on average, 2.12x faster executions compared to state-of-the-art methods.

## REFERENCES

- [1] A. DeHon, "The density advantage of configurable computing," *Computer*, vol. 33, no. 4, pp. 41–49, 2000.
- [2] F. Bouwens, M. Berekovic, A. Kanstein, and G. Gaydadjiev, "Architectural exploration of the adres coarse-grained reconfigurable array," in *Reconfigurable Computing: Architectures, Tools and Applications*, P. C. Diniz, E. Marques, K. Bertels, M. M. Fernandes, and J. M. P. Cardoso, Eds. Berlin, Heidelberg: Springer Berlin Heidelberg, 2007, pp. 1–13.
- [3] S. A. Chin, N. Sakamoto, A. Rui *et al.*, "CGRA-ME: A unified framework for CGRA modelling and exploration," in *2017 IEEE 28th International Conference on Application-specific Systems, Architectures and Processors (ASAP)*, 2017, pp. 184–189.
- [4] T. K. Bandara, D. Wijerathne, T. Mitra, and L.-S. Peh, "Revamp: a systematic framework for heterogeneous cgra realization," in *Proceedings of the 27th ACM International Conference on Architectural Support for Programming Languages and Operating Systems*, ser. ASPLOS '22. New York, NY, USA: Association for Computing Machinery, 2022, p. 918–932. [Online]. Available: <https://doi.org/10.1145/3503222.3507772>
- [5] S. Das, D. Rossi, K. J. M. Martin, P. Coussy, and L. Benini, "A 142mops/mw integrated programmable array accelerator for smart visual processing," in *2017 IEEE International Symposium on Circuits and Systems (ISCAS)*, 2017, pp. 1–4.
- [6] Z. Li, D. Wijerathne, X. Chen, A. Pathania, and T. Mitra, "Chordmap: Automated mapping of streaming applications onto cgra," *IEEE Transactions on Computer-Aided Design of Integrated Circuits and Systems*, vol. 41, no. 2, pp. 306–319, 2022.
- [7] R. Prabhakar, Y. Zhang, D. Koeplinger *et al.*, "Plasticine: A reconfigurable architecture for parallel patterns," in *2017 ACM/IEEE 44th Annual International Symposium on Computer Architecture (ISCA)*, 2017, pp. 389–402.
- [8] B. Mei, S. Vernalde, D. Verkest, H. De Man, and R. Lauwereins, "Exploiting loop-level parallelism on coarse-grained reconfigurable architectures using modulo scheduling," in *2003 Design, Automation and Test in Europe Conference and Exhibition*, 2003, pp. 296–301.

- [9] B. Mei, “Dresc: A retargetable compiler for coarse-grained reconfigurable architectures,” in *2002 IEEE International Conference on Field-Programmable Technology, 2002.(FPT). Proceedings*. IEEE, 2002, pp. 166–173.
- [10] S. Friedman, A. Carroll, B. Van Essen, B. Ylvisaker, C. Ebeling, and S. Hauck, “Spr: an architecture-adaptive cgra mapping tool,” in *Proceedings of the ACM/SIGDA International Symposium on Field Programmable Gate Arrays*, ser. FPGA ’09. New York, NY, USA: Association for Computing Machinery, 2009, p. 191–200. [Online]. Available: <https://doi.org/10.1145/1508128.1508158>
- [11] G. Gobieski, S. Ghosh, M. Heule *et al.*, “Riptide: A programmable, energy-minimal dataflow compiler and architecture,” in *2022 55th IEEE/ACM International Symposium on Microarchitecture (MICRO)*, 2022, pp. 546–564.
- [12] K. J. M. Martin, “Twenty years of automated methods for mapping applications on cgra,” in *2022 IEEE International Parallel and Distributed Processing Symposium Workshops (IPDPSW)*, 2022, pp. 679–686.
- [13] J. Lou, X. Gao, Y. Mao *et al.*, “An agile deploying approach for large-scale workloads on cgra-cpu architecture,” in *2024 Design, Automation and Test in Europe Conference Exhibition (DATE)*, 2024, pp. 1–6.
- [14] C. Sunny, S. Das, K. J. M. Martin, and P. Coussy, “Hardware based loop optimization for cgra architectures,” in *Applied Reconfigurable Computing. Architectures, Tools, and Applications*, S. Derrien, F. Hannig, P. C. Diniz, and D. Chillet, Eds. Cham: Springer International Publishing, 2021, pp. 65–80.
- [15] Z. E. Rakossy, A. Acosta-Aponte, T. G. Noll, G. Ascheid, R. Leupers, and A. Chattopadhyay, “Design and synthesis of reconfigurable control-flow structures for cgra,” in *2015 International Conference on ReConfigurable Computing and FPGAs (ReConFig)*, 2015, pp. 1–8.
- [16] D. Voitsechov and Y. Etsion, “Single-graph multiple flows: energy efficient design alternative for gpgpus,” in *Proceeding of the 41st Annual International Symposium on Computer Architecture*, ser. ISCA ’14. IEEE Press, 2014, p. 205–216.
- [17] M. Karunaratne, D. Wijerathne, T. Mitra, and L.-S. Peh, “4D-CGRA: Introducing Branch Dimension to Spatio-Temporal Application Mapping on CGRAs,” in *2019 IEEE/ACM International Conference on Computer-Aided Design (ICCAD)*, Nov. 2019, pp. 1–8.
- [18] J. Deng, X. Tang, J. Zhang *et al.*, “Towards efficient control flow handling in spatial architecture via architecting the control flow plane,” in *Proceedings of the 56th Annual IEEE/ACM International Symposium on Microarchitecture*, ser. MICRO ’23. New York, NY, USA: Association for Computing Machinery, 2023, p. 1395–1408. [Online]. Available: <https://doi.org/10.1145/3613424.3614246>
- [19] G. Gobieski, A. O. Atli, K. Mai, B. Lucia, and N. Beckmann, “Snafu: An ultra-low-power, energy-minimal cgra-generation framework and architecture,” in *2021 ACM/IEEE 48th Annual International Symposium on Computer Architecture (ISCA)*, 2021, pp. 1027–1040.
- [20] M. Karunaratne, A. K. Mohite, T. Mitra, and L.-S. Peh, “Hycube: A cgra with reconfigurable single-cycle multi-hop interconnect,” in *2017 54th ACM/EDAC/IEEE Design Automation Conference (DAC)*, 2017, pp. 1–6.
- [21] R. R. Álvarez, B. Denkinger, J. Sapriza, J. M. Calero, G. Ansaloni, and D. A. Alonso, “An open-hardware coarse-grained reconfigurable array for edge computing,” in *Proceedings of the 20th ACM International Conference on Computing Frontiers*, 2023, pp. 391–392.
- [22] D. Wijerathne, Z. Li, M. Karunaratne, L.-S. Peh, and T. Mitra, “Morpher: An open-source integrated compilation and simulation framework for cgra,” in *Fifth Workshop on Open-Source EDA Technology (WOSET)*, 2022.
- [23] T. Miyamori and K. Olukotun, “Remarc: Reconfigurable multimedia array coprocessor,” *IEICE Transactions on information and systems*, vol. 82, no. 2, pp. 389–397, 1999.
- [24] M. B. Taylor, J. Kim, J. Miller *et al.*, “The raw microprocessor: A computational fabric for software circuits and general-purpose programs,” *IEEE micro*, vol. 22, no. 2, pp. 25–35, 2002.
- [25] A. V. Aho, M. S. Lam, R. Sethi, and J. D. Ullman, *Compilers: Principles, Techniques, and Tools (2nd Edition)*. USA: Addison-Wesley Longman Publishing Co., Inc., 2006.
- [26] S. Das, K. J. M. Martin, P. Coussy, D. Rossi, and L. Benini, “Efficient mapping of cdfg onto coarse-grained reconfigurable array architectures,” in *2017 22nd Asia and South Pacific Design Automation Conference (ASP-DAC)*, 2017, pp. 127–132.
- [27] S. Das, K. J. M. Martin, D. Rossi, P. Coussy, and L. Benini, “An energy-efficient integrated programmable array accelerator and compilation flow for near-sensor ultralow power processing,” *IEEE Transactions on Computer-Aided Design of Integrated Circuits and Systems*, vol. 38, no. 6, pp. 1095–1108, 2019.
- [28] C. Tirelli, J. Sapriza, R. Rodríguez Álvarez *et al.*, “Sat-based exact modulo scheduling mapping for resource-constrained cgras,” *J. Emerg. Technol. Comput. Syst.*, vol. 20, no. 3, Aug. 2024. [Online]. Available: <https://doi.org/10.1145/3663675>
- [29] C. Lattner, M. Amini, U. Bondhugula *et al.*, “Mlir: Scaling compiler infrastructure for domain specific computation,” in *2021 IEEE/ACM International Symposium on Code Generation and Optimization (CGO)*, 2021, pp. 2–14.
- [30] Y. Luo, C. Tan, N. B. Agostini *et al.*, “Ml-cgra: An integrated compilation framework to enable efficient machine learning acceleration on cgras,” in *2023 60th ACM/IEEE Design Automation Conference (DAC)*, 2023, pp. 1–6.
- [31] T. Yu, O. Ragheb, S. Wicklund, and J. Anderson, “Mlir-to-cgra: A versatile mlir-based compiler framework for cgras,” in *2024 IEEE 35th International Conference on Application-specific Systems, Architectures and Processors (ASAP)*, 2024, pp. 184–192.
- [32] A. Chin and J. Anderson, “An Architecture-Agnostic Integer Linear Programming Approach to CGRA Mapping,” in *2018 55th ACM/IEEE Design Automation Conference (DAC)*, Jun. 2018, pp. 1–6.
- [33] C. Tirelli, L. Ferretti, and L. Pozzi, “Sat-mapit: A sat-based modulo scheduling mapper for coarse grain reconfigurable architectures,” in *2023 Design, Automation and Test in Europe Conference Exhibition (DATE)*, 2023, pp. 1–6.
- [34] D. Liu, Y. Xia, J. Shang, J. Zhong, P. Ouyang, and S. Yin, “E2EMap: End-to-End Reinforcement Learning for CGRA Compilation via Reverse Mapping,” in *2024 IEEE International Symposium on High-Performance Computer Architecture (HPCA)*, Mar. 2024, pp. 46–60.

- [35] T. Ruschke, L. J. Jung, D. Wolf, and C. Hochberger, "Scheduler for inhomogeneous and irregular cgras with support for complex control flow," in *2016 IEEE International Parallel and Distributed Processing Symposium Workshops (IPDPSW)*, 2016, pp. 198–207.
- [36] C. Sunny, S. Das, K. J. M. Martin, and P. Coussy, "Crepe: Concurrent reverse-modulo-scheduling and placement for cgras," *IEEE Transactions on Parallel and Distributed Systems*, vol. 35, no. 7, pp. 1293–1306, 2024.
- [37] K. Han, J. Ahn, and K. Choi, "Power-efficient predication techniques for acceleration of control flow execution on cgra," *ACM Trans. Archit. Code Optim.*, vol. 10, no. 2, May 2013. [Online]. Available: <https://doi.org/10.1145/2459316.2459319>
- [38] B. Yuan, J. Zhu, X. Man *et al.*, "Dynamic-ii pipeline: Compiling loops with irregular branches on static-scheduling cgra," *IEEE Transactions on Computer-Aided Design of Integrated Circuits and Systems*, vol. 41, no. 9, pp. 2929–2942, 2022.
- [39] B. Yuan, L. Liu, J. Zhu, and X. Man, "Compiling loops with branches on static-scheduling cgra," in *2021 IEEE 4th International Conference on Computer and Communication Engineering Technology (CCET)*, 2021, pp. 290–294.
- [40] M. Hanzeh, A. Shrivastava, and S. Vrudhula, "Branch-aware loop mapping on cgras," in *2014 51st ACM/EDAC/IEEE Design Automation Conference (DAC)*, 2014, pp. 1–6.
- [41] Z. E. Rakossy, A. Acosta-Aponte, T. G. Noll, G. Ascheid, R. Leupers, and A. Chattopadhyay, "Design and synthesis of reconfigurable control-flow structures for cgra," in *2015 International Conference on ReConfigurable Computing and FPGAs (ReConFig)*, 2015, pp. 1–8.
- [42] M. A. Watkins, T. Nowatzki, and A. Carno, "Software transparent dynamic binary translation for coarse-grain reconfigurable architectures," in *2016 IEEE International Symposium on High Performance Computer Architecture (HPCA)*, 2016, pp. 138–150.
- [43] M. Suzuki, Y. Hasegawa, Y. Yamada *et al.*, "Stream applications on the dynamically reconfigurable processor," in *Proceedings. 2004 IEEE International Conference on Field- Programmable Technology (IEEE Cat. No.04EX921)*, 2004, pp. 137–144.
- [44] V. Dadu, J. Weng, S. Liu, and T. Nowatzki, "Towards general purpose acceleration by exploiting common data-dependence forms," in *Proceedings of the 52nd Annual IEEE/ACM International Symposium on Microarchitecture*, ser. MICRO '52. New York, NY, USA: Association for Computing Machinery, 2019, p. 924–939. [Online]. Available: <https://doi.org/10.1145/3352460.3358276>
- [45] Y. Wang, C. Tirelli, L. Orlandic *et al.*, "An mlir-based compilation framework for cgra application deployment," *Applied Reconfigurable Computing, Architectures, Tools, and Applications*, 2025.
- [46] S. Hack, D. Grund, and G. Goos, "Register allocation for programs in SSA-form," in *Compiler Construction: 15th International Conference, CC 2006, Vienna, Austria, March 30-31, 2006. Proceedings 15*. Springer, 2006, pp. 247–262.
- [47] L.-N. Pouchet, "Polybench: The polyhedral benchmark suite," 2012, accessed: 2025-03-24. [Online]. Available: <https://github.com/MatthiasReisinger/PolyBenchC-4.2.1>
- [48] M. Guthaus, J. Ringenberg, D. Ernst, T. Austin, T. Mudge, and R. Brown, "Mibench: A free, commercially representative embedded benchmark suite," in *Proceedings of the Fourth Annual IEEE International Workshop on Workload Characterization. WWC-4 (Cat. No.01EX538)*, 2001, pp. 3–14.